

Effect of compatibilization on the properties of polyamide 66/polypropylene (75/25 wt/wt) blends

J. Duvall, C. Sellitti, V. Topolkaev, A. Hiltner* and E. Baer

Department of Macromolecular Science and Center for Applied Polymer Research, Case Western Reserve University, Cleveland, OH 44106, USA

and C. Myers

Amoco Chemical Company, Research and Development, Naperville, IL 60566, USA

(Received 5 November 1993; revised 24 February 1994)

Blends consisting of a polyamide 66 (PA) matrix (75 wt%) and a dispersed isotactic polypropylene (PP) phase were prepared by extrusion with anhydride-grafted isotactic polypropylene compatibilizers, one of high anhydride content (HAC, 2.7 wt% grafted maleic anhydride) and one of low anhydride content (LAC, 0.2 wt% grafted anhydride). HAC and LAC had similar effects on PP domain size and tensile properties at equal loadings, unlike the anhydride concentration dependency that had been reported for high PP content blends. As compatibilizer loading increased from 0 wt% to 7.5 wt%, a skin/core injection-moulded morphology gradient diminished, PP domain size decreased to less than 1 μm , tensile strain increased and microscale deformation of the PP phase progressed from debonding to particle drawing and debonding to fibril fracture. The PP phase deformation mode depends on the interfacial strength as compared to the PP domain strength. HAC and LAC are postulated to behave similarly because of sufficient reactivity with PA and similar surface coverage by HAC-*g*-PA and LAC-*g*-PA. Interfacial strength is postulated to increase with decreasing particle size because of increasing surface/volume ratio at relatively constant surface coverage.

(Keywords: compatibilization; polyamide 66; polypropylene)

INTRODUCTION

Polyamides are frequently blended with lower modulus polymers such as rubbers¹⁻⁴ or polyolefins^{5,6} to improve material properties. The addition of polypropylene (PP) lowers water absorption and reduces material cost. This can be achieved without drastically changing the mechanical properties if there is adequate chemical or physical interaction between the components. However, polyamides and PP require a compatibilizing agent to promote PP dispersion and interfacial adhesion. Specific techniques for compatibilizing these particular polymers with maleated polypropylene and other functionalized polyolefins have been described⁷⁻¹¹. Although addition of PP does not supertoughen the polyamide in this case, substantial toughness can be retained through the use of appropriate coupling agents.

Two critical parameters for toughening polyamides are particle size and interfacial adhesion, and it has been shown that polyamide rubber blends require a particle size less than 1 μm to achieve supertoughness¹⁻⁴. Dispersion of the minor phase may be determined in blends of incompatible components by the coupling agent or by rheological effects such as the relative viscosities of the two components^{12,13}. Changing the particle size and/or adhesion alters the deformation mode of the soft inclusion; specifically, whether the particle debonds or plastically deforms with the matrix. The

transition from particle debonding to drawing corresponds to improved blend properties.

In a previous study¹⁴, two maleic anhydride grafted isotactic polypropylene compatibilizers, one of high anhydride content (HAC) and one of low anhydride content (LAC), were used to compatibilize PP-rich blends of PP with polyamide 66 (PA). The very different blend properties that resulted with these compatibilizers were explained in terms of the higher propensity of LAC to co-crystallize with the PP matrix¹⁵. In the present study, the same two compatibilizers are used in PA-rich blends of the same PP and PA resins, so that now the matrix is PA and the dispersed phase is PP. The focus of the study is on the mechanisms of compatibilization and the effects of interfacial strength on tensile properties of the blends.

EXPERIMENTAL

Materials

Blends of polypropylene (PP) and polyamide 66 (PA) were supplied by the Amoco Chemical Company. The polyamide was Dupont Zytel 101 with an M_w of 29 000 and an M_n of 14 000. Titration of the end-groups gave a value of 3×10^{-5} equivalents of amine per gram. The polyamide was dried in a -30°C dewpoint oven for 12–16 h at 71°C before compounding. The polypropylene was stabilized Amoco isotactic homopolymer with a melt flow rate of 3.5 g per 10 min, an M_w of 356 000 and an M_n of 71 000. The PP melted at 164°C with a crystallinity

* To whom correspondence should be addressed

of 50%. Blends of PA and PP were compatibilized with two different, relatively low molecular weight isotactic poly(propylene-graft-maleic anhydride) (PP-*g*-MA) compatibilizers. Both LAC and HAC were semicrystalline, the melting temperatures being respectively 160°C (38% crystallinity) and 155°C (36% crystallinity). The compatibilizers were vacuum dried at 100°C for 16 h before compounding.

Molecular weights of the compatibilizers were determined by gel permeation chromatography (g.p.c.) and the anhydride contents were measured by n.m.r., FTi.r. and titration. The low anhydride compatibilizer (LAC) had an M_w of 135 000 and an M_n of 42 500 with an average of one anhydride group per chain (0.2 wt% anhydride). The high anhydride compatibilizer (HAC) had an M_w of 52 100 and an M_n of 16 100 with an average of six anhydride groups per chain (2.7 wt% anhydride). While LAC had much less grafted anhydride, it also had a molecular weight approximately three times higher than that of HAC. Both LAC and HAC were characterized by g.p.c. and by FTi.r. after vacuum drying and also after precipitation from hot xylene into acetone followed by vacuum drying. No difference in molecular weight distribution or grafted anhydride content was found between the non-precipitated and precipitated samples. The differential scanning calorimetry (d.s.c.) melting behaviour was also the same. Therefore, LAC and HAC were presumed to be randomly grafted and not mixtures of highly grafted oligomer and polypropylene.

Methods

The blend components were compounded in a nitrogen-purged barrel (45/1 L/D) in a Werner-Pfleiderer ZSK-30 extruder at 285°C, dried in a -60°C dewpoint oven and injection moulded using a multispecimen mould and a temperature of 277°C throughout the barrel. The injection pressure was 16 MPa, the back pressure was 0.34 MPa and the mould cavity temperature was 65°C. The specimens were then stored in sealed containers with a desiccant and dried in a vacuum at 80°C for 3–4 days before testing.

Blend compositions used in this study were prepared with 1.25 wt%, 2.5 wt%, 3.75 wt% and 7.5 wt% compatibilizer. The anhydride concentration in blends compatibilized with HAC was more than 10 times higher than in blends compatibilized with the same amount of LAC, owing to the larger number of anhydride groups on HAC chains and the lower molecular weight. The amount of PP in the blends was adjusted so that PP plus compatibilizer was 25 wt%, while the PA remained constant at 75 wt%.

Injection-moulded dogbone specimens (type 1 ASTM D638) 3.15 mm thick and 12.5 mm wide were used to characterize morphology and mechanical behaviour. Undeformed specimens were cryogenically fractured parallel or perpendicular to the injection-moulding direction after submersion in liquid nitrogen for 1 h. Fracture surfaces were coated with 60 Å (1 Å = 0.1 nm) of gold and the domain morphology was observed using a JEOL 840A scanning electron microscope. Tensile bars with a V notch (45°) 2.5 mm in depth were fractured at ambient temperature using a crosshead displacement speed on the Instron of 2 mm min⁻¹. The fracture surfaces were coated with 60 Å of gold in order to observe the microdeformation processes in the scanning electron microscope.

Uniaxial tensile tests of unnotched specimens were conducted at room temperature with a strain rate of 5% min⁻¹. Tensile strength was taken as either the maximum stress or the yield stress. When debonding stresses were to be determined, a single acoustic emission sensor, a Physical Acoustic Corporation (PAC) R15 with a resonant frequency of 160 kHz, was fixed to the centre of the specimen with high vacuum silicone grease as a coupling medium. The acoustic emission (AE) generated during deformation was analysed with a PAC Spartan AT system. The AE threshold was set at 29 dB.

RESULTS AND DISCUSSION

Morphology

Polypropylene was poorly dispersed in polyamide 66 without a compatibilizer. The PP particle size ranged from 2 µm to 20 µm with an average of about 10 µm. Poor interfacial adhesion was evident from the large voids left on the fracture surface where the particles had separated from the matrix and the smooth surfaces of the exposed PP particles (*Figure 1a*). The addition of 2.5 wt% LAC reduced the average particle size in the blend to 3 µm (*Figure 1b*). Similarly, addition of 2.5 wt% HAC reduced the average PP particle size to 2.5 µm (*Figure 1c*). Interfacial adhesion also seemed to improve with addition of 2.5 wt% of either compatibilizer because some of the PP particles on the fracture surfaces had adhered matrix material. Better dispersion and improved interfacial adhesion were attributed to formation of a PP-*g*-MA/PA copolymer by reaction of anhydride groups with terminal amine groups of PA during melt mixing. The dispersion improved when the copolymer stabilized the interface by forming an interfacial layer between PP particles and the PA matrix. Improved adhesion depended on strong chemical or physical interactions with particles and matrix.

Anisotropy of the phase morphology and gradients in morphology through the thickness of the 3.2 mm thick tensile specimens were examined in cross-sections parallel to the mould-filling direction. Two examples, blends with 2.5 wt% and 7.5 wt% LAC, are shown in *Figure 2*. The micrographs illustrate the decrease in particle size with increasing compatibilizer content, and also suggest better adhesion in the blend with higher compatibilizer content since the particles in the 7.5 wt% LAC blend appear to be more deeply embedded in the matrix. A morphology gradient was especially apparent in the blend with lower compatibilizer content. Near the edge, the PP particles in the blend with 2.5 wt% LAC were highly elongated in the injection direction. The aspect ratio gradually decreased through the thickness from 8–10 near the edge until the particles were essentially spherical in the centre. Particle size also decreased from the edge to the centre. The morphology gradient in the blend with higher compatibilizer content was less pronounced and there was less variation in particle size. Near the edge, the elongated PP particles in the blend with 7.5 wt% LAC had an aspect ratio of about 3. In addition to the morphology gradient illustrated in *Figure 2*, both blends had a very thin skin where the particles were platelet shaped that is not visible in the micrographs.

The average particle size in the centre is plotted in *Figure 3* as a function of the amount of compatibilizer to show that the particle size depended on the amount

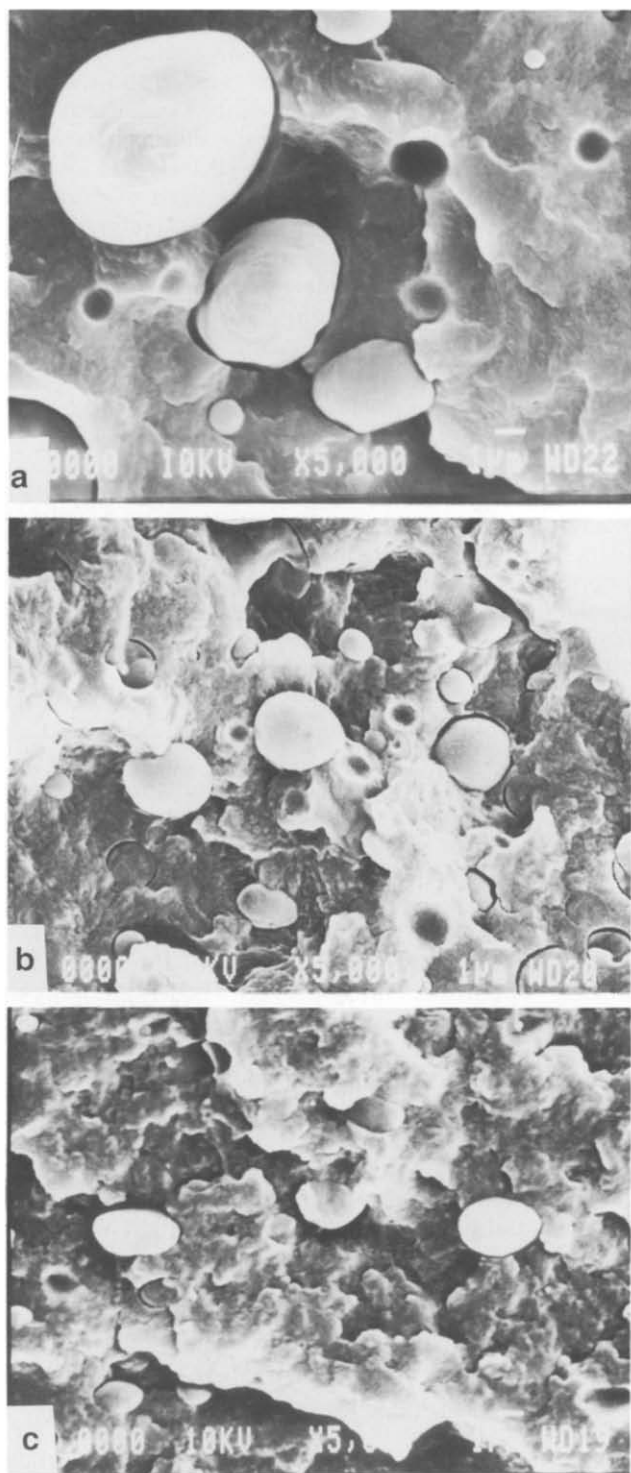


Figure 1 Morphologies of PP/PA 75/25 wt/wt blends: (a) uncompatibilized; (b) with 2.5 wt% LAC; (c) with 2.5 wt% HAC

of compatibilizer but was not strongly affected by whether LAC or HAC was used in the blend. If it is assumed that the PP-*g*-MA/PA copolymer is located at the interface between the two phases with complete penetration of the two phases, the average interfacial area stabilized per compatibilizer molecule (A) can be estimated from¹⁶

$$A = \frac{3\Phi M_n}{RW_c N} \quad (1)$$

where Φ is the volume fraction of the dispersed phase, M_n is the number average molecular weight of the compatibilizer, R is the particle radius, W_c is the mass of compatibilizer per unit volume of blend and N is Avogadro's number. The calculated values of surface area stabilized per compatibilizer molecule in *Table 1* are estimates only. With this qualification, the average interfacial area per compatibilizer molecule is remarkably similar for LAC and HAC, and is not strongly affected by compatibilizer content. However, cognizance that the calculation assumed that 100% of the compatibilizer stabilized the interface was needed in the subsequent interpretation of these numbers.

The copolymer formed by LAC and PA may have been close to a PP/PA diblock structure. Since most of the compatibilizer chains of LAC had a single terminal anhydride group, coupling of LAC and PA would have occurred at the chain ends with formation of a diblock copolymer, according to the generally accepted reaction mechanism. The assumption that all LAC molecules reacted to form block copolymer and were located at the interface (*Figures 4a* and *4b*) was supported by the concentration independence of the calculated interfacial area stabilized per compatibilizer molecule and the large amine/anhydride ratio in the LAC blends. The average value of 180 \AA^2 could then, as a first approximation, be taken as the area stabilized by each reacted anhydride. The average surface area of 180 \AA^2 for LAC was smaller than that obtained previously for PP-*g*-MA/polyamide 6 copolymer (260 \AA^2)¹⁰, but larger than the minimum suggested for a diblock copolymer completely penetrating the two phases (50 \AA^2)¹⁶.

The HAC molecule had on average six anhydride groups and potentially could have formed a copolymer with multiple grafts by reacting with more than one amine; nevertheless, the area stabilized by an HAC molecule was slightly less than that stabilized by LAC. While this could have suggested that on average the HAC copolymer bridged the interface and completely penetrated the two phases in a manner similar to the LAC copolymer, it was also possible that several anhydrides on some HAC molecules reacted and the resulting comb-shaped copolymer was spread out on the interface, while most of the HAC was elsewhere. If on average three of the six anhydride groups on an HAC molecule reacted¹⁴, it was estimated from the surface area that about one in six HAC molecules would have contributed to stabilizing the interface when the HAC content was 1.25 wt% and one in four when the HAC content increased to 7.5 wt%. Considering the approximate nature of these calculations, the most significant result was that only a fraction of the HAC, perhaps of the order of 20%, contributed to stabilization of the interface. It would have been surprising if the remaining HAC was unreacted since the amine/anhydride ratio was as high as 6.6 and greater than 1 for all the PA-rich blends with HAC. A possible explanation for the apparent low efficiency of HAC in PA-rich blends is that copolymer from HAC molecules with the most grafting sites was dispersed in the PA phase, while graft copolymer from HAC molecules with fewer anhydrides penetrated both phases and stabilized the interface (*Figures 4c* and *4d*). With fewer than the average six anhydrides per molecule, this copolymer would have been more like copolymer from LAC.

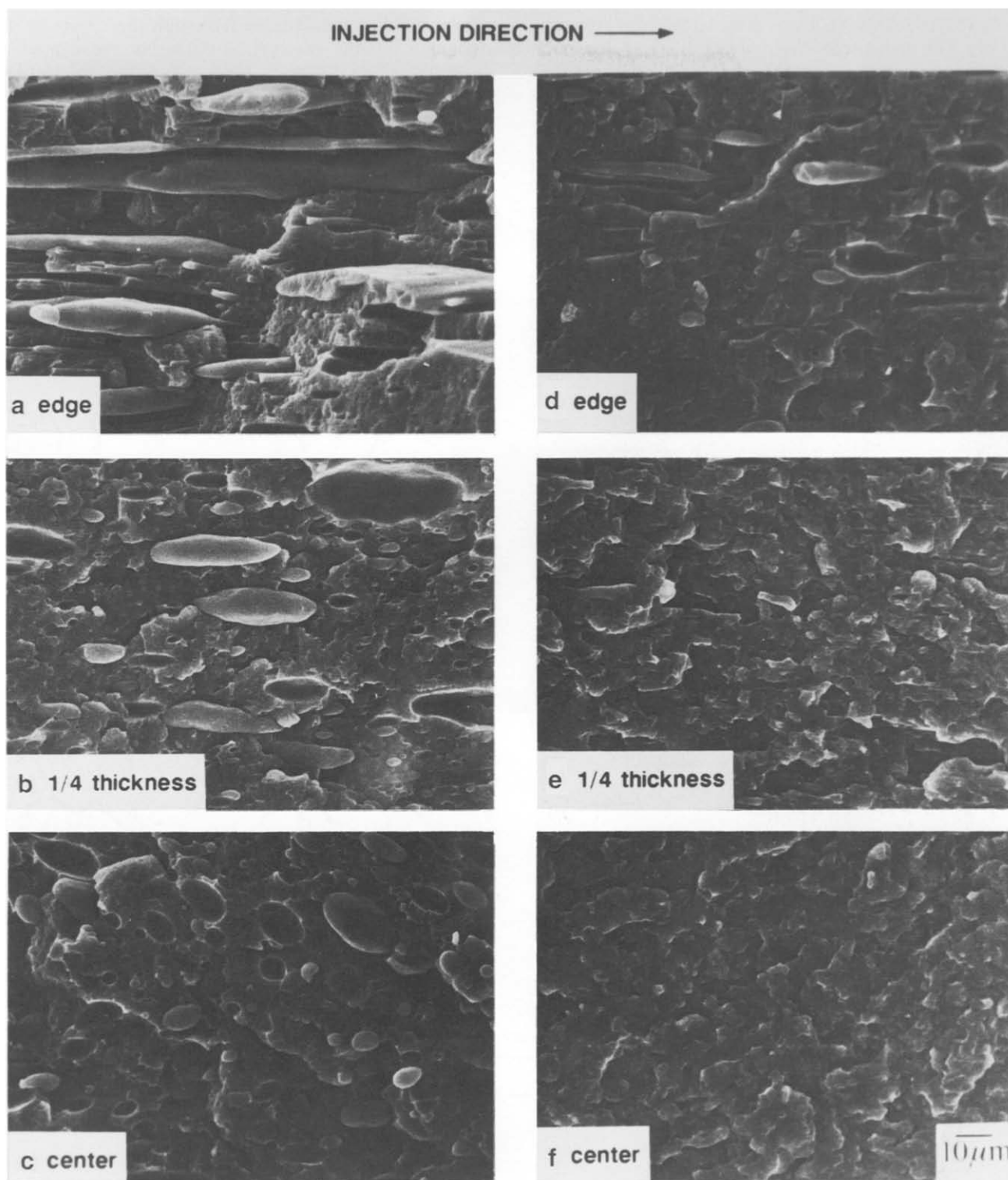


Figure 2 Morphology gradient parallel to the injection-moulding direction: (a–c) blend with 2.5 wt% LAC; (d–f) blend with 7.5 wt% LAC

Mechanical behaviour

The tensile stress/strain behaviour of the uncompatibilized materials is shown in *Figure 5*. Dry PA exhibited a tensile yield strength of 80 MPa and fractured at about 25% strain after necking. Blending 25 wt% PP with PA reduced the tensile strength to 50 MPa and decreased the fracture strain to 10%. Necking was not observed in the blend. The loss in mechanical properties is characteristic of an incompatible blend.

Stress/strain curves of the compatibilized blends are compared in *Figure 6*. The fracture strains were slightly

higher with HAC than with LAC, but in general the two compatibilizers had about the same effect on the mechanical properties. Addition of compatibilizer resulted in an increase in tensile strength to about 62 MPa. Assuming good adhesion, the tensile strength calculated by the rule of mixtures was 66 MPa. Although the tensile strength of the compatibilized blends did not depend on the amount of compatibilizer, the fracture strain gradually increased as the compatibilizer content increased from 1.25 wt% to 7.5 wt%. Blends with 7.5 wt% compatibilizer, either LAC or HAC, exhibited necking before they

fractured at a strain that was close to the fracture strain of PA. The increased tensile strength of all the compatibilized blends suggested that even the smallest amount of compatibilizer improved the interfacial strength sufficiently to prevent particle debonding before yielding. However, debonding of the PP particles during yielding was indicated in the blends with 1.25 wt% compatibilizer by the low fracture strain, comparable to the fracture strain of the uncompatibilized blend. The gradually increasing fracture strain with increasing compatibilizer content was attributed to improved interfacial strength.

Since the tensile yield strength of the PP particles was lower than the tensile strength of the PA matrix, an indication of the interfacial strength was derived from the extent to which the PP particles were deformed when the blend fractured. Figure 7 shows the fracture surfaces

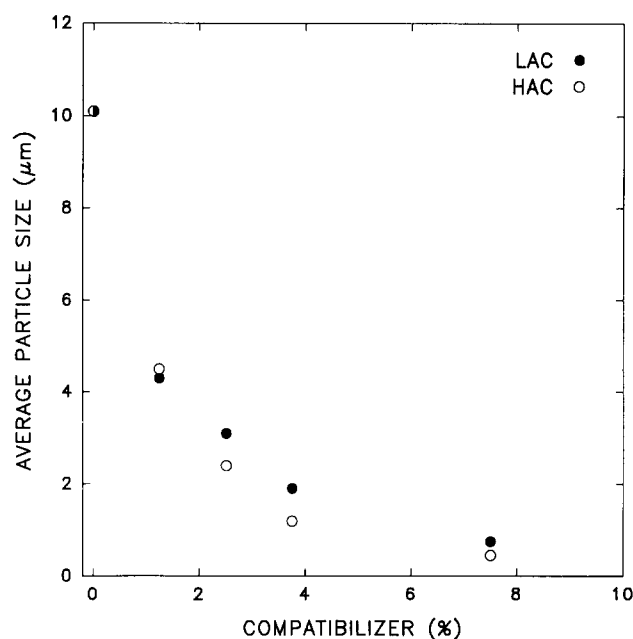


Figure 3 Average polypropylene particle size as a function of compatibilizer content

from notched tensile tests. Although there were striking changes in the fracture surfaces as the amount of compatibilizer increased, the results with LAC and HAC were virtually the same. On the fracture surfaces of the blends with 1.25 wt% compatibilizer, undeformed PP particles with smooth surfaces had debonded from the surrounding PA which had pulled out and fibrillated. This indicated that in these blends the interfacial strength was less than the tensile yield strength of PP. In contrast, the PP particles on the fracture surfaces of the blends with 7.5 wt% compatibilizer were highly drawn. The thin tapering ends of the drawn-out PP fibrils suggested that

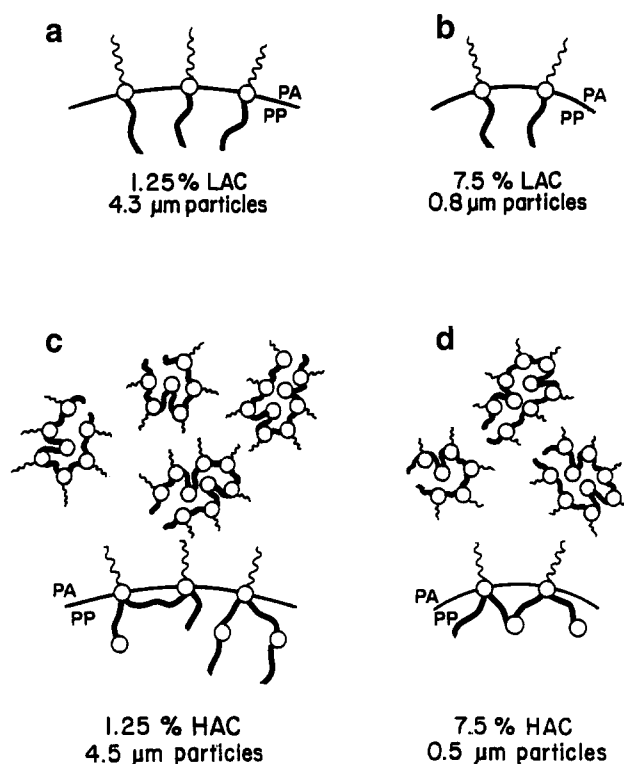


Figure 4 Schematic representation of interface stabilization: (a) 1.25 wt% LAC; (b) 7.5 wt% LAC; (c) 1.25 wt% HAC; (d) 7.5 wt% HAC

Table 1 Average sizes of particles and areas stabilized per molecule of compatibilizer

Compatibilizer content (wt%)	PP/PA (25/75 wt/wt)						PP/PA (75/25 wt/wt)					
	LAC			HAC			LAC			HAC		
	<i>R</i> ^a	<i>D</i> ^b	<i>A</i> ^c	<i>R</i>	<i>D</i>	<i>A</i>	<i>R</i>	<i>D</i>	<i>A</i>	<i>R</i>	<i>D</i>	<i>A</i>
0.80										3.4	0.8	552
1.00										2.7	0.7	566
1.25	88.2	4.3	214	6.6	4.5	88						
2.00										1.4	0.6	398
2.50	44.1	3.2	144	3.3	2.3	86	14.7	2.4	161	1.1	0.5	353
3.75	29.4	1.8	170	2.2	1.0	131	9.8	1.8	137	0.7	0.4	265
7.50	14.7	0.8	192	1.1	0.5	131	4.9	1.3	95	0.4	0.4	133
11.25							3.3	0.7	118	0.2	0.4	88
15.00							2.5	0.6	103			
20.00							1.8	0.6	93			
25.00							1.5	0.5	82			

^a *R* = amine/anhydride ratio

^b *D* = particle diameter (μm)

^c *A* = surface area stabilized per compatibilizer molecule (Å²)

the fibrils fractured rather than debonded during final separation. Therefore, the interfacial strength in these blends was higher than the true fracture stress of PP.

Intermediate behaviour was observed on the fracture surfaces of blends with 2.5 wt% compatibilizer. While some undeformed PP particles were observed together with particles that had drawn out and fractured, most of the particles had yielded, drawn partially and then debonded. There did not appear to be a correlation between particle size and whether the particle debonded or drew out. Thus, some of the largest particles were drawn out while some of the smallest particles were undeformed, indicating that they had debonded. The

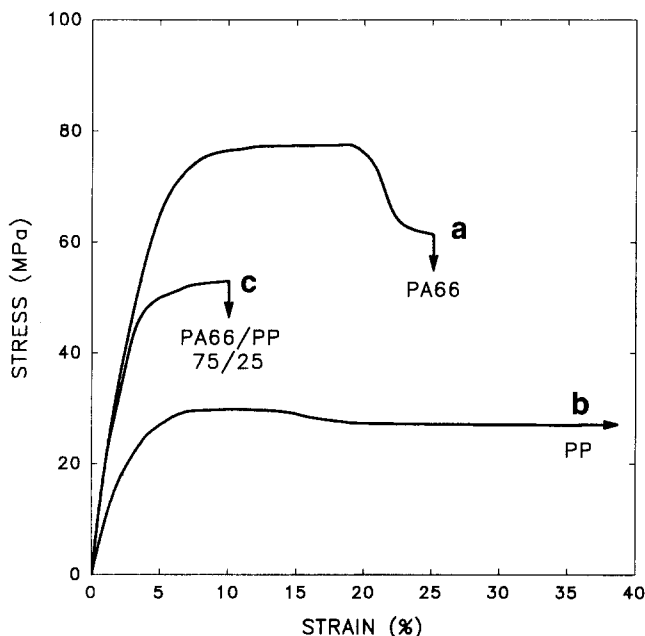


Figure 5 Stress/strain curves of control materials: (a) PA; (b) PP; (c) PA/PP (75/25 wt/wt)

interfacial strength of a PP particle that yielded and subsequently debonded would have been greater than the tensile yield strength of PP but less than the true fracture stress of PP. The fracture surfaces of the blends with 3.75 wt% compatibilizer were similar except that no undeformed PP particles were observed. Most of the particles were drawn and debonded, but a few had drawn and fractured at mid-fibril.

There was no evidence that the specific interfacial strength increased with compatibilizer content; on the contrary, the remarkable consistency of the calculated interfacial area per compatibilizer molecule suggested that the interaction remained essentially constant. Even so, the interfacial strength might have increased as the particles became smaller because of the higher surface/volume ratio, thus accounting for the change from particle debonding to particle drawing. While the surface/volume ratio determines elastic debonding¹⁷, it is only speculation that a similar relationship exists for the plastic case. In this regard, it should be noted that there was no good correlation between particle size and particle failure mechanism when both modes were observed with the intermediate blend compositions. It thus appeared that the distribution of the compatibilizer was not necessarily uniform among the particles, a situation that would have resulted if some of the PP had been dispersed rheologically rather than by compatibilization. This would have created small PP particles with low interfacial strength.

Interfacial strength

The lower limit of interfacial strength in the PA/PP blends was that of the uncompatibilized blend. Since the tensile strength of the uncompatibilized blend was significantly lower than that predicted by the rule of mixtures, it was anticipated that debonding occurred before yielding. Debonding was detected by monitoring the acoustic emission during tensile testing of an unnotched specimen. *Figure 8a* shows the stress/strain

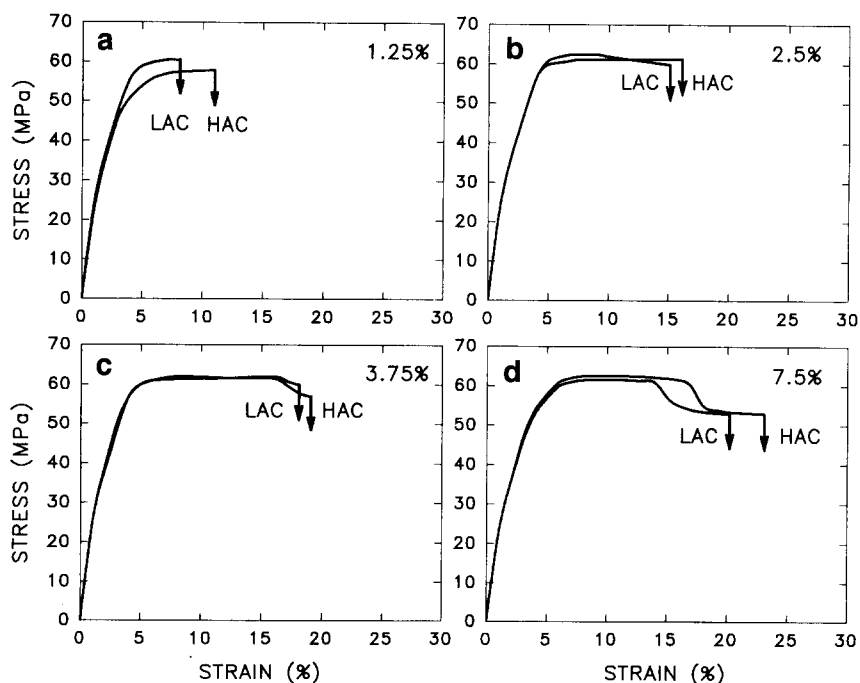


Figure 6 Stress/strain curves of blends compatibilized with (a) 1.25 wt%, (b) 2.5 wt%, (c) 3.75 wt% and (d) 7.5 wt% LAC and HAC

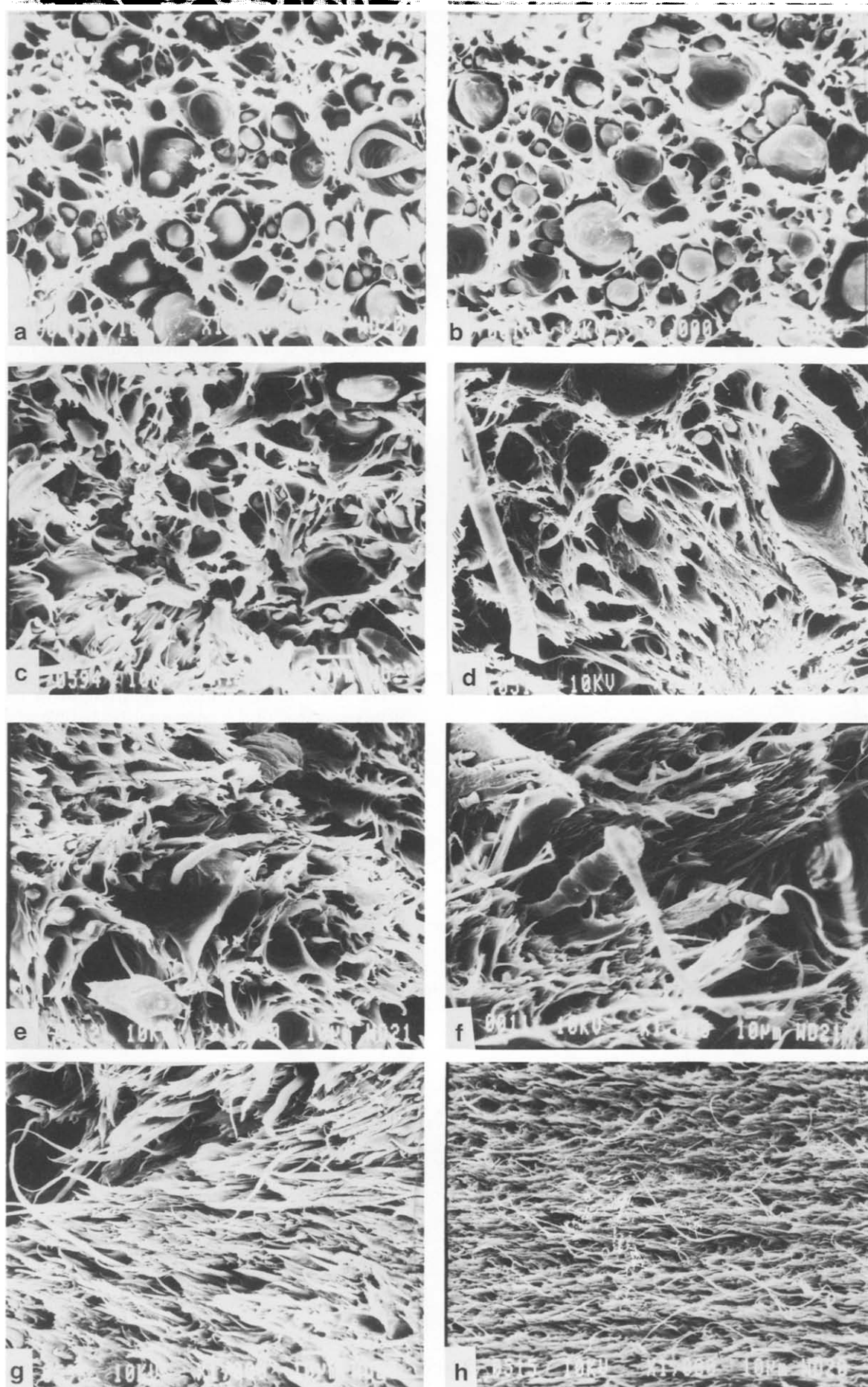


Figure 7 Tensile fracture surfaces of compatibilized blends: (a) 1.25 wt% LAC; (b) 1.25 wt% HAC; (c) 2.5 wt% LAC; (d) 2.5 wt% HAC; (e) 3.75 wt% LAC; (f) 3.75 wt% HAC; (g) 7.5 wt% LAC; (h) 7.5 wt% HAC

curve together with the non-cumulative AE events for the uncompatibilized blend. The AE activity began at 1% strain and then diminished at 3% strain when the stress levelled off. The lower limit of the debonding stress (σ_d) was taken as 24.0 MPa, the applied stress at 1% strain when AE was first detected.

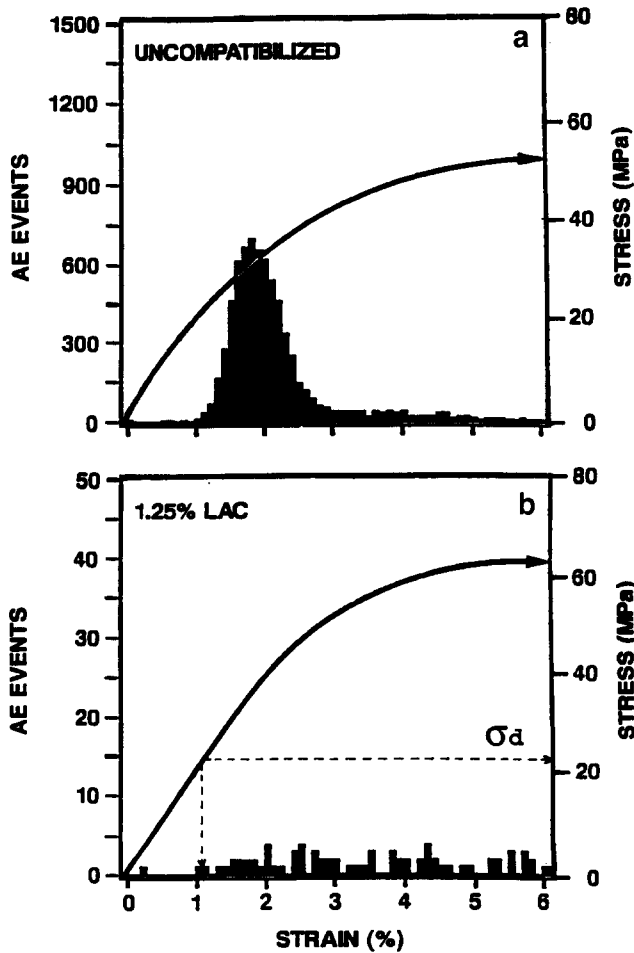


Figure 8 Acoustic emissions generated during tensile tests of (a) the uncompatibilized blend and (b) a blend compatibilized with 1.25 wt% LAC

Results of the same experiment performed on the blend with 1.25 wt% LAC are shown in Figure 8b. Here also AE was first detected at about 1% strain when the applied stress reached 24.0 MPa. However, AE events continued to be detected at a fairly constant rate after the stress levelled off. This suggested that the upper limit of the interfacial strength was slightly higher than the tensile yield strength of PP. Plastic debonding of the PP particles, i.e. debonding after the particles reached their tensile yield strength, was consistent with a tensile strength for the compatibilized blend close to that predicted by the rule of mixtures. Although the upper limit of the interfacial strength was slightly higher than the tensile yield strength, the PP particles did not appear deformed on the fracture surface because the strains were small. The distributions of elastic debonding and plastic debonding were the result of varying degrees of interfacial strength from particle to particle, and were attributed at least in part to non-uniform distribution of the compatibilizer.

Estimates of the interfacial strength as a function of particle size are summarized in Figure 9. Three distinct regions of interfacial strength corresponding to the three particle failure modes were defined: the debonding region where the interfacial strength was lowest; an intermediate region where particles were partially drawn and debonded; and finally a region where particles were drawn out and the fibrils fractured. The upper limit of the elastic debonding region was the tensile yield strength of PP ($\sigma_{t,PP} = 28$ MPa), below which the interfacial strength was not sufficient to cause deformation of the particles. Elastic debonding of the particles in the uncompatibilized blend was detected by acoustic emission and was also indicated by the low tensile strength of the blend. At the other extreme, the lower limit of the fibril fracture region was the true fracture stress of PP ($\sigma_{f,PP}$), below which the interfacial strength could not sustain drawing to fracture of the PP fibril. To obtain an approximate value for this limit, the cross-sectional area of a PP fibril was estimated from micrographs and a fracture load calculated from the true fracture stress of PP, determined experimentally to be 210 MPa. The fibril fracture load was then divided

SUMMARY OF FAILURE PROCESSES
PP/PA (25/75)

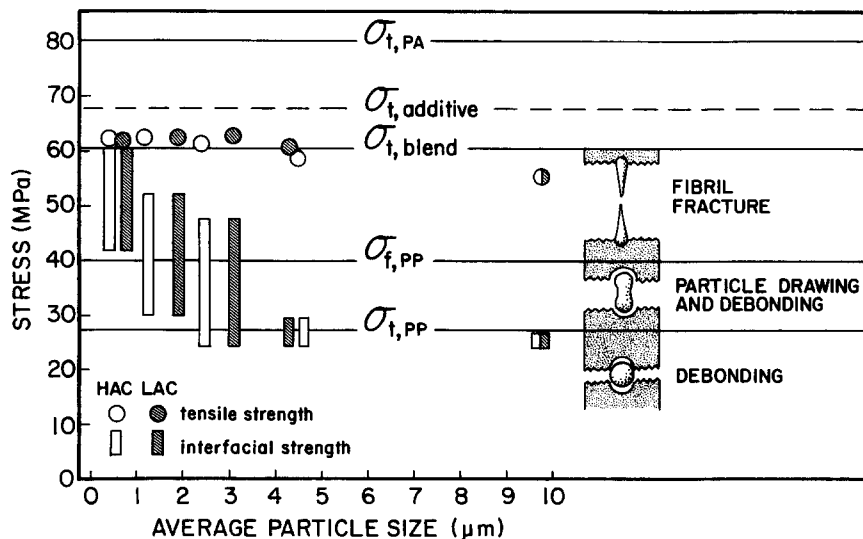


Figure 9 Interfacial strength as a function of particle size indicating the region of each particle failure mode: debonding, particle drawing and fibril fracture

by the surface area of the PP particle that remained adherent, estimated to be one third. This resulted in a value of 40 MPa as the minimum interfacial strength for PP particles to fail by fibril fracture.

The debonding mode was observed in blends with 1.25 wt% compatibilizer. Both elastic debonding and plastic debonding were detected by acoustic emission. The increased tensile strength compared to the uncompatibilized blend also indicated that the particles were load bearing at the yield point. Therefore, the bars in *Figure 9* that represent the range in interfacial strength extend above the tensile yield strength of PP. The blends with 2.5 wt% compatibilizer had a small fraction of debonded particles with little or no plastic deformation. The majority of the particles appeared drawn but final separation occurred by debonding rather than fibril fracture. The interfacial strength for such a particle was between the tensile yield strength of PP and the true fracture stress of PP. The remaining fraction of particles appeared to fracture in the fibril, in which case the interfacial strength was above 40 MPa. The bars in *Figure 9* are intended to signify the relative frequencies of the three failure modes. Since no debonded particles were observed on the fracture surfaces of blends with 3.75 wt% compatibilizer, the bars in *Figure 9* are shown only in the partial drawing with debonding and fibril fracture regions. Only fractured fibrils were observed on the fracture surfaces of the blends with 7.5 wt% compatibilizer, this being indicated by a bar that began above 40 MPa and extended to the tensile strength of the blend ($\sigma_{t,blend} = 61.5$ MPa).

The particle failure mode did not significantly influence the tensile strength of the compatibilized blends, which suggested that even when the particles failed by debonding the interfacial strength was close to the tensile yield strength of PP. On the other hand, the particle failure mode did significantly influence the fracture strain. Debonding of large PP particles in the blends with low compatibilizer content created critical-size flaws, and the likelihood of a critical-size flaw decreased as the particles became smaller. Furthermore, when the particle failure mode changed from debonding to plastic deformation, flaw formation leading to premature fracture was suppressed, while bridging PP fibrils retarded crack propagation during final separation.

Comparison of PA-rich and PP-rich blends

Included in *Table 1* are data previously reported for a PP-rich blend composition (25 wt% PA) compatibilized with LAC and HAC¹⁴. In this case the particle size referred to PA particles in the PP matrix. Again, the interfacial area stabilized per compatibilizer molecule was calculated from equation (1). The largest value of 160 Å² per molecule obtained for the PP-rich blend compatibilized with 2.5 wt% LAC is comparable to values calculated for PA-rich blends with LAC. The decreasing surface area as the LAC content increases in the PP-rich blend parallels the decrease in the amine/anhydride ratio, and was attributed to less than complete reaction of anhydride; the unreacted LAC molecules were probably dispersed in the PP phase. The compatibilization efficiency of LAC was consistent with a diblock structure for the copolymer formed from LAC and PA, and furthermore suggested that compatibilization of PA-rich and PP-rich blends with LAC could be viewed in an analogous way,

with the block copolymer located at the interface and completely penetrating the two phases. In both cases, the expected effect on mechanical properties was observed; in particular, the tensile strength of the compatibilized blends approached that predicted by the rule of mixtures, and the fracture strain increased with compatibilizer content.

A good compatibilizer should function in two ways: firstly, it should reduce the interfacial energy between phases to permit a finer dispersion in the melt; and secondly, it should provide good adhesion between the phases for better mechanical properties in the solid state. The compatibilization efficiency of HAC depended on whether PP was the continuous phase or the dispersed phase. When PP was the continuous phase, small amounts of HAC were very effective in dispersing PA. The area stabilized by HAC was as high as 560 Å² per molecule, which then decreased gradually as the amount of HAC increased. It was speculated that HAC molecules had multiple grafts, and it was estimated that three of the six anhydrides reacted. It was argued that once an HAC molecule came into contact with a PA particle and one anhydride reacted, the close proximity of other anhydride groups on the chain made it more likely that they would react and the grafted molecule would spread on the interface. The gradually decreasing surface area reflected a smaller fraction of reacted HAC molecules as the amine/anhydride ratio decreased to less than 1. Owing to the tendency of HAC to phase separate from PP, unreacted HAC probably accumulated in the interface region. Crystallization of HAC as a separate phase was thought to be responsible for poor interfacial strength. As a consequence, the HAC-compatibilized PP-rich blends never achieved the ductility of the LAC-compatibilized blends; moreover, the ductility decreased as the amount of HAC increased.

In PA-rich blends, the dispersion and property enhancements achieved with LAC and HAC were almost equivalent on a weight basis, although the anhydride concentration of HAC was an order of magnitude higher than that of LAC. Unlike PP-rich blends with HAC, the amine/anhydride ratio was greater than 1 in all PA-rich blends with HAC and this also favoured a high reaction efficiency for HAC. To explain the apparent low efficiency of HAC in PA-rich blends, it was proposed that the copolymer from HAC molecules with the most grafting sites was dispersed in the PA phase, while the graft copolymer from HAC molecules with fewer anhydrides penetrated both phases and stabilized the interface. The copolymer dispersed in PA had no noticeable deleterious effect on the mechanical properties, while the copolymer that stabilized the interface imparted essentially the same mechanical properties to the blend as the LAC copolymer.

CONCLUSIONS

A low anhydride compatibilizer (LAC) and a high anhydride compatibilizer (HAC) both improved the dispersion of polypropylene (PP) in polyamide 66 (PA). The injection-moulded morphology gradient through the thickness diminished as the compatibilizer content was increased from 0 wt% to 7.5 wt%. The compatibilizers had similar effects on particle size and tensile properties at equal loadings, unlike the anhydride concentration dependency that had been observed for PP-rich blends.

It was speculated that only a fraction of the HAC contributed to stabilization of the interface, while the most highly grafted HAC molecules were dispersed in the PA phase.

Since the tensile yield strength of the dispersed PP phase was lower than the tensile strength of the matrix, the PP deformation mode depended on the interfacial strength as compared to the PP domain strength. As the PP particle size decreased from 10 μm in the uncompatibilized blend to less than 1 μm with 7.5 wt% LAC or HAC, the microscale deformation mode progressed from debonding to particle drawing and debonding to fibril fracture. Interfacial strength was postulated to increase with decreasing particle size because of the increasing surface/volume ratio at relatively constant surface coverage.

ACKNOWLEDGEMENTS

The authors thank the Amoco Chemical Company for financial support of this work and for supplying the materials. The Amoco Corporate Research Laboratory provided FTIR, n.m.r. and titrimetric analysis of the compatibilizers. Titration of the polyamide for amine end-groups was performed by R. Keske of Amoco Performance Products Inc. Polymer blend extrusion, moulding and purification of analytical samples were

performed by members of the Polymer Applications Group, especially M. Wreschinsky.

REFERENCES

- 1 Wu, S. *Polymer* 1985, **26**, 1855
- 2 Margolina, A. and Wu, S. *Polymer* 1988, **29**, 2170
- 3 Fukui, T., Kikuchi, Y. and Inoue, T. *Polymer* 1991, **32**, 2367
- 4 Takeda, Y., Keskkula, H. and Paul, D. R. *Polymer* 1992, **33**, 3173
- 5 Hobbs, S. Y., Bopp, R. C. and Watkins, V. H. *Polym. Eng. Sci.* 1983, **23**, 380
- 6 Padwa, A. R. *Polym. Eng. Sci.* 1992, **32**, 1703
- 7 Ide, F. and Hasegawa, A. *J. Appl. Polym. Sci.* 1974, **18**, 963
- 8 Park, S. J., Kim, B. K. and Jeong, H. M. *Eur. Polym. J.* 1990, **26**, 131
- 9 Willis, J. M., Caldas, V. and Favis, B. D. *J. Mater. Sci.* 1991, **26**, 4742
- 10 Hosoda, S., Kojima, K., Kanda, Y. and Aoyagi, M. *Polym. Networks Blends* 1991, **1**, 51
- 11 Holsti-Miettinen, R. and Seppälä, J. *Polym. Eng. Sci.* 1992, **32**, 868
- 12 Wu, S. *Polym. Eng. Sci.* 1987, **27**, 335
- 13 Park, I., Keskkula, H. and Paul, D. R. *J. Appl. Polym. Sci.* 1992, **45**, 1313
- 14 Duvall, J., Sellitti, C., Myers, C., Hiltner, A. and Bauer, E. *J. Appl. Polym. Sci.* 1994, **52**, 195
- 15 Duvall, J., Sellitti, C., Myers, C., Hiltner, A. and Baer, E. *J. Appl. Polym. Sci.* 1994, **52**, 207
- 16 Paul, D. R. in 'Polymer Blends' (Eds D. R. Paul and S. Newman), Vol. 2, Academic Press, New York, 1978, Ch. 12
- 17 Zhuk, A. V., Knunyants, N. N., Oshmyan, V. G., Topolkaev, V. A. and Berlin, A. A. *J. Mater. Sci.* 1993, **28**, 4595